Improvement of sensitivity of graphene photodetector by creating bandgap structure*

Ni-Zhen Zhang(张倪侦)[1], Meng-Ke He(何孟珂)[1], Peng Yu(余鹏)[1,†], and Da-Hua Zhou(周大华)[2,‡]

[1] *Chongqing Key Laboratory of Photo-Electric Functional Materials, College of Physics and Electronic Engineering, Chongqing Normal University, Chongqing* 401331, *China*

[2] *Chongqing Key Laboratory of Multi-scale Manufacturing Technology, Chongqing Institute of Green and Intelligent Technology, Chinese Academy of Sciences, Chongqing* 400714, *China*

(Received 18 June 2017; revised manuscript received 29 July 2017; published online 29 September 2017)

Graphene has aroused large interest in optoelectronic applications because of its broad band absorption and ultrahigh electron mobility. However, the low absorption of 2.3% seriously limits its photoresponsivity and restricts the relevant applications. In this paper, a method to enhance the sensitivity of graphene photodetector is demonstrated by introducing electron trapping centers and creating a bandgap structure in graphene. The carrier lifetime obviously increases, and more carriers are collected by the electrodes. Compared with intrinsic graphene detector, the defective graphene photodetector possesses high photocurrent and low-driving-voltage, which gives rise to great potential applications in photodetector area.

Keywords: graphene, photodetector, photocurrent, bandgap

PACS: 68.65.Pq, 78.67.Wj, 81.05.ue **DOI:** 10.1088/1674-1056/26/11/116803

1. Introduction

The detection of photons plays an important role in imaging, spectroscopy, and optical communications. Conventionally, detectors made from silicon crystalline and complementary metal oxide semiconductor (CMOS) are always applied to light sensing. However, the integration of bulk semiconductor-based on-chip detectors has faced many challenges, such as front-end changes in COMS processing, spectral response range limit by the material bandgap, and the response speed corresponding to the carrier mobility.[1] In recent years, ultrathin films have become attractive for photodetection,[2,3] which are used as the photo-electric responsive material in these nanostructure detectors: they are not only compatible with conventional silicon electronics, but also make flexible devices.

Graphene, a kind of two-dimensional honeycomb lattice material with a unique structure, has aroused wide interest as a new generation semiconductor material. It has a high charge carrier mobility and can absorb photons in range from the visible to the infrared. Both properties embody its potential applications in broadband optical modulator and ultra-broad band photodetector. Indeed, since the first ultrafast graphene detector was fabricated in 2009,[5] many experiments on graphene photodetector have been carried out, including the basic photodetection mechanisms and related applications.[6–9]

Despite many attractive features for graphene photodetector, the low optical absorption in graphene film results in a low external quantum efficiency. Moreover, its high carrier mobility brings about a fast recombination time for the photo-generated carriers, which also limits the number of collected carriers at the electrodes. To solve these problems, various methods have been suggested. Firstly, a usual method is to design a special cavity. For example, Marco Furchi placed the graphene in a Fabry–Perot microcavity, which can enhance the absorption to more than 60%,[10] or in some other cavity structures, e.g., graphene integrated with photonic crystal cavity or silicon waveguide.[11,12] However, a special cavity corresponds to a special resonance frequency, which means that the detection bands are limited. In addition, integrating the graphene with metallic plasmonic nanostructures could greatly enhance the photocurrent.[13] Researchers also combined graphene with other two-dimensional materials to fabricate a hybrid or hetero structure, such as graphene–MoS_2,[14] graphene–perovskite,[15] graphene–Bi_2Te_3,[16] graphene–PbS quantum dots,[17] and MoS_2–graphene–WSe_2 heterostructure.[18] However, no matter whether the plasmon resonance enhancement or the hybrid structure is used, the methods always have their own disadvantages, such as a much longer responsive time than intrinsic graphene photodetector, or just a narrow detection band, or the device is very difficult to fabricate. To increase the photoresponsivity, besides increasing the absorption efficient, one can also increase the lifetime of the photogenerated carriers. In this respect, by introducing defect midgap states band and a bandgap into graphene, high photoresponsivity as 8.61 A/W has been obtained.[19]

*Project supported by the National Natural Science Foundation of China (Grant No. 51271210), the Chongqing Municipal Research Program of Basic Research and Frontier Technology, China (Grant No. cstc2015jcyjBX0039), and the Foundation for the Creative Research Groups of Higher Education of Chongqing Municipality, China (Grant No. CXTDX201601016).

†Corresponding author. E-mail: pengyu@cqnu.edu.cn

‡Corresponding author. E-mail: zhoudahua@cigit.ac.cn

© 2017 Chinese Physical Society and IOP Publishing Ltd

In this paper, we demonstrate a sensitive photodetector by introducing electron trapping centers in graphene. Firstly, the chemical vapor deposition (CVD)-grown graphene was transferred onto the SiO_2/Si substrate, and then etched the film into ribbons. After the electrodes is fabricated, a nano-scale thin Ti sacrificial layer is deposited on the device. Finally, to remove the Ti layer, a mixed solution (HF and H_2O_2) is used as a wet etching solution. Therefore, a quantum dot-like array structure is produced on the graphene (here, it is called defective graphene), and many electron trapping centers are formed. By this process, photo-generated carriers have a longer lifetime, and it is found that the defective graphene photodetector has a high photoresponsivity and low driving voltage, which proves the potential applications of graphene in photodetection.

2. Experiments

Graphene growth is performed by the conventional CVD technique. Briefly speaking, a copper foil was first pretreated by being immersed in 5% nitric acid solution, and then annealed in a hydrogen atmosphere at high temperature to clear the surface contamination. Methane was introduced as a carbon source with a growth temperature of about 1050 °C. Finally, the sample was cooled to room temperature in hydrogen atmosphere. After growth, the graphene was transferred onto the Si/SiO_2 (300 nm SiO_2) substrate by a wet-transfer technique.[20] In the transfer process, a thin layer of PMMA (4 wt% PMMA in ethyllactate) was first coated on the top of graphene, with a rotation speed of 6000 rpm for 40 s. To dry the PMMA layer, the sample was baked at 120 °C for 10 min. Then, the graphene-PMMA-Cu sample was rinsed in H_2O/HCl/H_2O_2, and deionized water respectively. Next, the Cu foil was etched, leaving the graphene supported on the PMMA membrane. Graphene/PMMA film was then transferred onto Si/SiO_2 substrate. Finally, the PMMA was dissolved in acetone.

After being transferred, the graphene film was fabricated into a photodetector by the following process as shown in Fig. 1. Firstly, to pattern the graphene, a PMMA layer was coated on the graphene, that was followed by the photolithography technique and a directional plasma oxygen etching technique in sequence. The resist was then removed by immersing the sample in acetone. Then, the source and the drain electrodes (Cr/Au: 5 nm/40 nm) were obtained by standard photolithography and lift-off technique. Next, the patterned graphene device was covered by a 2-nm-thick Ti film by the magnetron sputtering technique. The defective graphene was formed by etching the Ti sacrificial layer, using hydrofluoride, hydrodioxide (H_2O_2) and deionized water with a volume ratio of 1:1:200. The etching time is about 2 min. At the same time, a photodetector was fabricated using the CVD graphene directly, which is named pristine graphene.

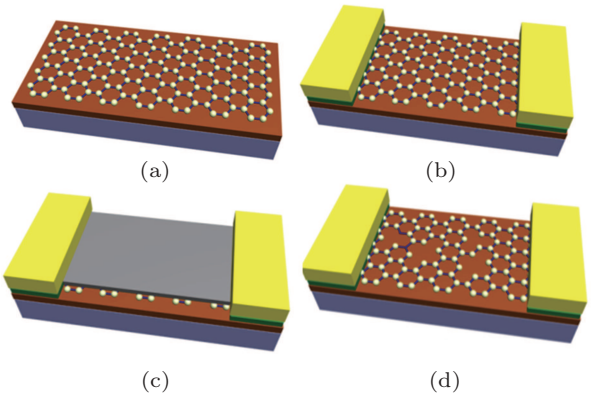


Fig. 1. (color online) Fabrication process of the defective graphene based photodetector: (a) transfer graphene, (b) graphene photodetector, (c) cover layer Ti, and (d) defective photodetector.

The single-layer nature of the graphene film was confirmed by Raman spectroscopy (inVia Reflex) with a 532 nm laser. In addition, the structure of the graphene detector was characterized by high-resolution scanning electron microscope (SEM; JSM-7800F). The photoelectric response measurements were carried out by a standard direct current (DC) technique. Electric measurements on the photodetector were performed on a station connected to Keithley semiconductor analyzer SCS4200. To investigate the device photoconductivity, a diode laser ($\lambda = 635$ nm) and a white light source (xenon lamp) were used respectively. In our experiment, the photocurrent response (I–t curve) at low driving voltage was measured at an electrochemical workstation. All the measurements were performed at room temperature.

3. Results and discussion

Figure 2 illustrates the growing and transferred graphene. Figure 2(a) shows the early stages of single crystal graphene growing on the Cu foil, and Fig. 2(b) is the grown graphene transferred on the silicon substrate. In order to understand the number of graphene layers, Raman spectroscopy is used to identify it. The two most intense peaks observed in graphene are G peak ($\sim$1582 cm^{-1}) and 2D peak ($\sim$2700 cm^{-1}), which are due to the double generated zone center E_{2g} mode and second order zone-boundary phonons.[21] To identify the layers of graphene, the intensity ratio of 2D peak to G peak is calculated. As reported in Ref. [21], only the intensity of 2D peak is twice that of G peak, the graphene is monolayer. In this experiment, it is found that most part of the area of the CVD grown graphene is monolayer, which shows a Raman spectrum as indicated in Fig. 3(a). In addition, some parts contain double or several layers, due to the intensity ratio between 2D peak and G peak being less than two as seen in Fig. 3(b). Finally, by deposing the Ti layer, one can find that the Raman spectrum shows a big difference:there exists almost no graphene Raman signal in Fig. 3(c). However, comparing the Raman spectrum of the etched monolayer graphene in Fig. 3(d) with the pristine ones in Figs. 3(a) and 3(b), we can find that the D peak owns a

much high intensity, and D′ peak appears in the G peak. The D peak is associated with graphene edge defects,[21] therefore, it can be concluded that quantum-dot structure arrays are formed on the surface of graphene. In this experiment, two kinds of photodetectors are prepared from CVD-grown monolayer graphene, namely pristine and defective graphene photodetector. The optical and SEM images of the detectors are shown in Figs. 4(a) and 4(b), respectively. It is reported in Ref. [19] that the graphene quantum dot (GQD) size is about 20.5 nm, however, since here the graphene is transferred by the wet method, and it is difficult to remove the PMMA completely by acetone, the graphene defects are not observed by the traditional atomic force microscope (AFM) experiments. The total light sensitive area of graphene film is 100 μm× 100 μm.

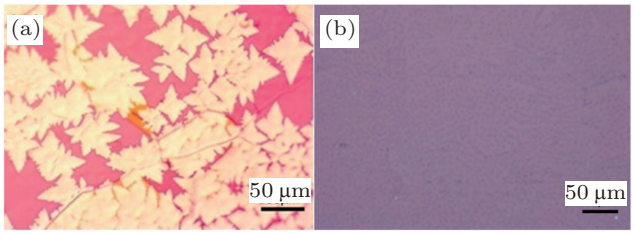


Fig. 2. (color online) (a) Early stages of graphene grown on the Cu foil. (b) SEM image of the surface morphology of transferred graphene onto SiO_2 after removing PMMA by acetone.

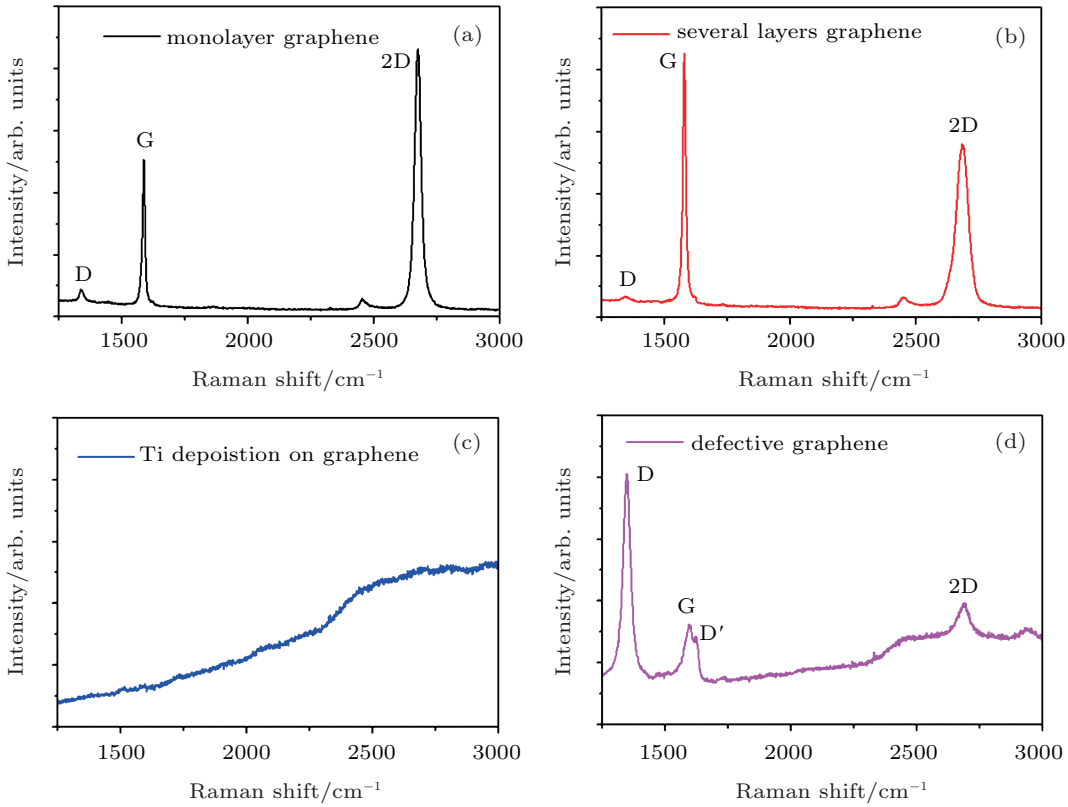


Fig. 3. (color online) Raman spectra of graphene of (a) monolayer graphene, (b) several layers of graphene, (c) Ti layer deposited on graphene, and (d) defective graphene.

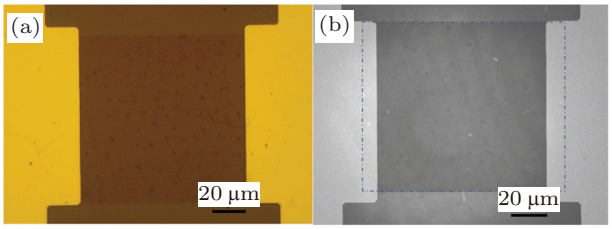


Fig. 4. (color online) (a) Optical and (b) SEM image of the fabricated graphene photodetector.

We further evaluate the electronic and photoelectric properties of the fabricated detectors with laser and white light sources, respectively. At first, *I*–*V* curves of the detectors under the illumination of white light are obtained. In Fig. 5, it is notable that comparing the photocurrent with dark current, both pristine and defective graphene photodetectors present nice light responsive characteristics. It should be pointed out that somewhat jitters appear in the *I*–*V* curve in Fig. 5(a). It is maybe due to charge and discharge process happening in the measurement, more detailed experiments are needed to clarify it. In addition, under the irradiation of 635 nm laser, the time-dependent photocurrent over several on–off periods of operation is shown in Fig. 6, with a voltage bias of 1 V. Clearly, the photocurrent of defective graphene detector reaches hundreds of nanoamperes, which is two orders of magnitude higher than that of the pristine one. Considering the fact that the excited laser power is 50 μW, the responsivities of the pristine and defective detectors are 0.22 mA/W and 290 mA/W, respec-

tively. In other words, with the Ti layer deposition and etching process, the quantum-dot-like graphene photodetector exhibits more excellent photoelectric response than that made of pristine graphene.

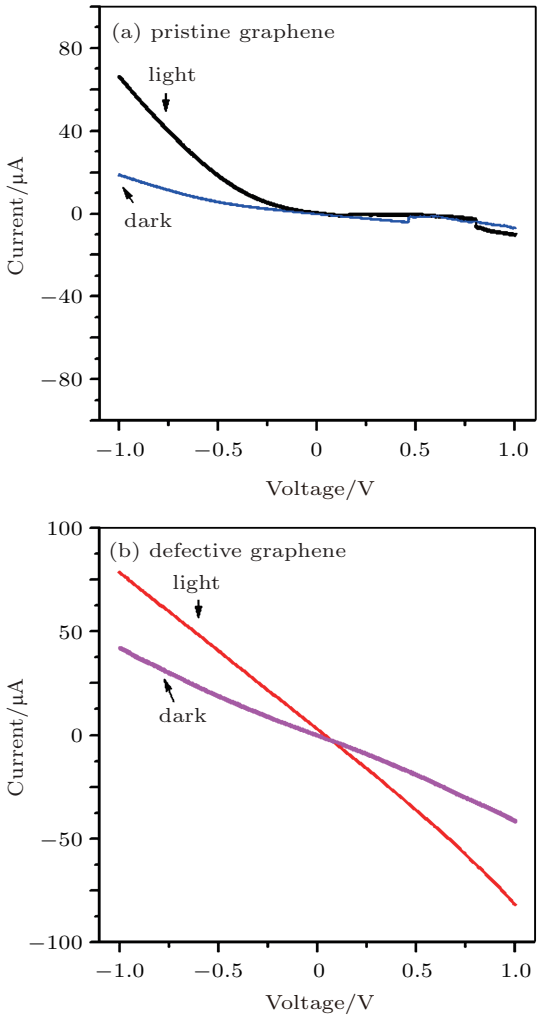


Fig. 5. (color online) The *I*–*V* curves of (a) the pristine graphene photodetector and (b) defective graphene photodetector under the irradiation of white light.

This higher photocurrent response can be attributed to the following mechanism: the CVD graphene sheet is first processed into quantum-dot-like structure, resulting in defect midgap state band and a bandgap as depicted in Fig. 7;[19] there are two ways of relaxing the photo-excited electrons to lower energy state in the conduction band, namely impact ionization (II) process and Auger recombination (AR); since the II process is more efficient than the AR process,[22] carrier multiplication occurs, which generates more secondary electrons in the conduction band; on the other hand, due to a bandgap created, more photo-excited and II-process-generated electrons can be trapped in the midgap state band;[19] therefore, more holes relating to the trapped electrons can be recirculated many times, and a photoconductive gain is achieved. In short, the carrier multiexciton effect, as well as the electron trapping in the midgap band is expected to contribute to the high photoresponse.

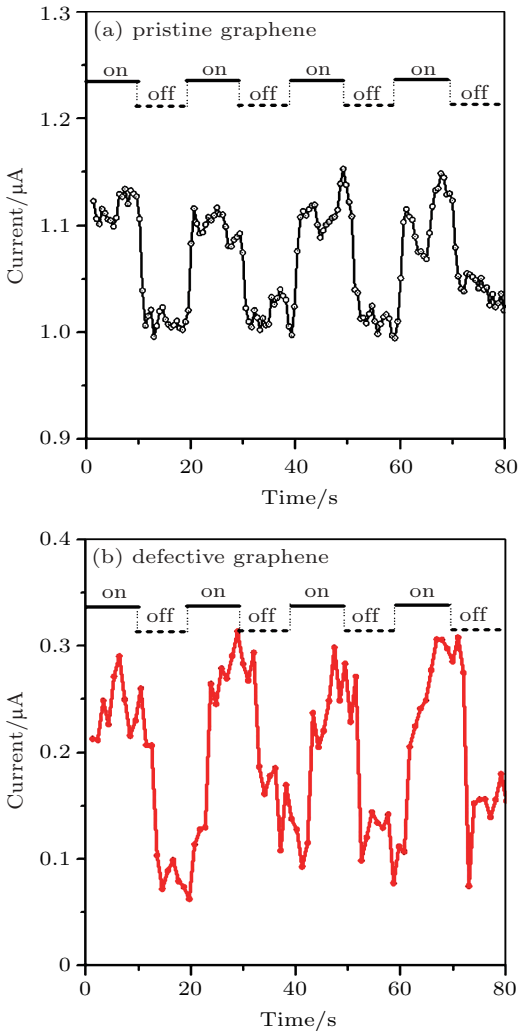


Fig. 6. (color online) Time-dependent photocurrent measurement of (a) the pristine graphene photodetector and (b) the defective graphene photodetector under the irradiation of 635 nm laser.

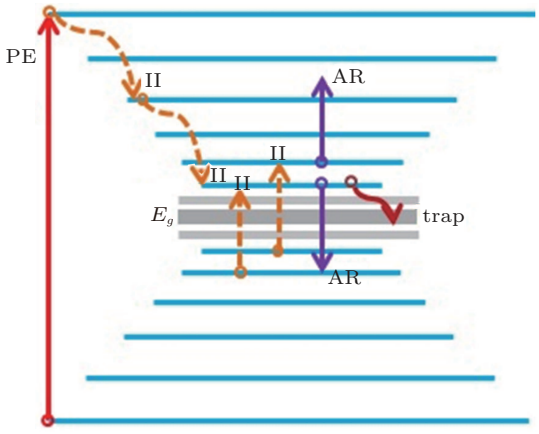


Fig. 7. (color online) Energy band diagram and concept of the defective graphene. PE: photo excited; II: impact ionization; AR: Auger recombination; Trap: free electrons trapped in midgap state band.

In addition, if the light source is white light, the GQD detector shows a high photocurrent response. There is even zero bias voltage between the two electrodes; about 2.8 μA photocurrent is obtained in the time-dependent measurements

(see Fig. 8). The responsivity of the defective detector (R_{ph}) can be evaluated from the following equation:[23]

$$R_{ph} = \frac{I_{ph}}{P_{in}},$$

where P_{in} is the power density of white light source, which is about 30 W/cm^2, and I_{ph} is the current of photocurrent. Therefore, one can obtain a responsivity of 0.93 mA/W with no bias voltage at the detector. Also, if 1 V bias voltage is used, a higher photocurrent is measured to be about 6.5 μA, with a dark current as high as about 78.5 μA. Comparing the photocurrents under the laser and white light source respectively, it could be concluded that the graphene layer has a high photoresponse in broadband.

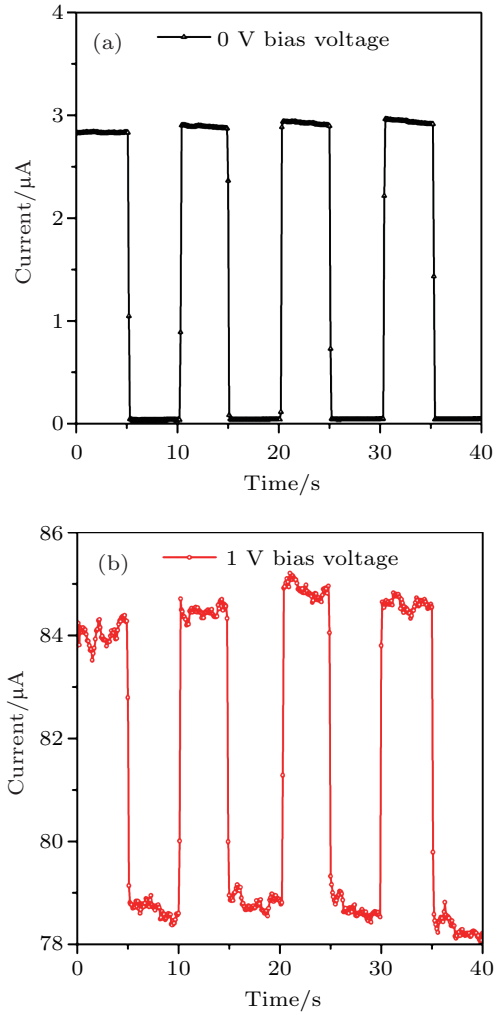


Fig. 8. (color online) Time-dependent photocurrent measurement of (a) the pristine graphene photodetector and (b) the defective graphene photodetector under the irradiation of white light.

4. Conclusions

In this work, we successfully fabricate a kind of photodetector based on CVD grown graphene. Via defect engineer process, namely titanium sacrificial layer fabrication method, the fabricated graphene photodetector shows a higher photoresponsivity than the pristine graphene photodetector. Compared with other methods, including the waveguide structure, the Fabry–Perot microcavity scheme, and plasmonic enhancement technique, this fabrication process is simple and repeatable. Additionally, since the fabricated photodetector shows a much high responsivity under the irradiation of white light source, especially a photocurrent response can be obtained at zero bias voltage, which means that this fabricated photodetector has wide applications in a broad spectral range.

References

[1] Shiue R J, Gao Y, Wang Y, Peng C, Robertson A D, Efetov D K, Assefa S, Koppens F H L, Hone J and Englund D 2015 *Nano Lett.* **15** 7288

[2] Koppens F H L, Mueller T, Avouris P, Ferrari A C, Vitiello M S and Polini M 2014 *Nat. Nanotechnol.* **9** 780

[3] Kin F M and Jie S 2016 *Nat. Phontonics* **10** 216

[4] Liu M, Yin X, Ulin-Avila E, Geng B, Zentgraf T, Ju L, Wang F and Zhang X 2011 *Nature* **474** 64

[5] Xia F, Mueller T, Lin Y, Valdes-Garcia A and Avouris P 2009 *Nat. Nanotechnol.* **4** 839

[6] Guo N, Hu W, Jiang T, Gong F, Luo W, Qiu W, Wang P, Liu L, Wu S, Liao L, Chen X and Lu W 2016 *Nanoscale* **8** 16065

[7] Wang Y B, Yin W H, Han Q, Yang X H, Ye H, Lv Q Q and Yin D D 2016 *Chin. Phys. B* **25** 118103

[8] Wang Y B, Yin W H, Han Q, Yang X H, Ye H, Lv Q Q and Yin D D 2017 *Chin. Phys. B* **26** 028101

[9] Du S, Lu W, Ali A, *et al.* 2017 *Adv. Mater.* **29** 1700463

[10] Furchi M, Urich A, Pospischil A, Lilley G, Unterrainer K, Detz H, Klang P, Andrews A M, Schrenk W, Strasser G and Mueller T 2012 *Nano Lett.* **12** 2773

[11] Shiue R J, Gan X, Gao Y, Li L, Yao X, Szep A, Walker D, Hone J and Englund D 2013 *Appl. Phys. Lett.* **103** 241109

[12] Pospischil A, Humer M, Furchi M M, Bachmann D, Guider R, Fromherz T and Mueller T 2013 *Nat. Photonics* **7** 892

[13] Liu Y, Cheng R, Liao L, Zhou H, Bai J, Liu G, Liu L, Huang Y and Duan X 2011 *Nat. Commun.* **2** 579

[14] Roy K, Padmanabhan M, Goswami S, Phanindra S T, Ramalingam G, Raghavan S and Ghosh A 2013 *Nat. Nanotechnol.* **8** 826

[15] Lee Y, Kwon J, Hwang E, Ra C H, Yoo W J, Ahn J H, Park J H and Cho J H 2015 *Adv. Mater.* **27** 41

[16] Qiao H, Yuan J, Xu Z, Chen C, Lin S, Wang Y, Song J, Liu Y, Khan Q, Hoh H Y, Pan C X, Li S and Bao Q 2015 *ACS Nano* **9** 1886

[17] Sun Z, Liu Z,Li J, Tai G A, Lau S P and Yan F 2012 *Adv. Mater.* **24** 5878

[18] Long M, Liu E, Wang P, *et al.* 2016 *Nano Lett.* **16** 2254

[19] Zhang Y, Liu T, Meng B, Li X, Liang G, Hu X and Wang Q J 2013 *Nat. Commun.* **4** 1811

[20] Jiao T, Wei D, Liu J, Sun W, Jia S, Zhang W, Feng Y, Shi H and Du C 2015 *Rsc Adv.* **5** 73202

[21] Ferrari A C, Meyer J C, Scardaci V, Casiraghi C, Lazzeri M, Mauri F, Piscanec S, Jiang D, Novoselov K S, Roth S and Geim A K 2006 *Phys. Rev. Lett.* **97** 187401

[22] Sukhovatkin V, Hinds S, Brzozowski L and Sargent E H 2009 *Science* **324** 1542

[23] Sun Z and Chang H 2014 *ACS Nano* **8** 4133